Ballistic Testing of Armor Panels Based on Aramid

Catalin Pirvu and Lorena Deleanu

Additional information is available at the end of the chapter

Abstract

Industry and market of ballistic protection materials and systems are characterized by a dynamic and competing succession of inventions for projectiles and protective systems. The requirements for the ballistic panels are many and complex, varying depending on the threat type, the required mobility in the tactical theater, and protection level. The safety degree, the price, and the dynamics of research in the field are also taken into account. This chapter underlines the necessity of testing ballistic protection panels made of LFT SB1 plus (multidirectional fiber fabrics, supplied by Teijin) against a certain threat in order to assess their resistance to this specific threat and the investigation of failure mechanisms in order to improve their behavior at ballistic impact. The models for ballistic impact are useful when they are particularly formulated for resembling the actual system projectile, target, and can be validated through laboratory experiments. Tests made on panels made of LFT SB1plus, according to NIJ Standard-0101.06-2008 gave good results for the panels made of 12 layers of this fabric, and the backface signature (BFS) was measured. The BFS upper tolerance limit of 24,441 mm recommends this system for protection level IIA, according to the abovementioned standard.

Keywords: ballistic impact, aramid fabrics, damage investigation

1. Introduction

Industry and market of ballistic protection materials and systems are characterized by a dynamic and competing succession of inventions for projectiles and protective systems. The requirements for the ballistic panels are many and complex, varying depending on the threat type, the required mobility in a tactical theater, and protection level. The safety degree, the price, and the dynamics of research in the field are also taken into account. The research on hit targets by a projectile characterized by more than 120 m/s is of high interest nowadays in several important domains, like army, navy, space systems, and nuclear one. The intensive

competition on polymeric, woven or not, fabrics and the growth of their market at a global level are factors that bust research toward efficient innovations, including the assembling technologies here.

The initial design of a protective system is supported by simulations using sophisticated codes that take into account the material characteristics under a high strain rate and particular processes characterizing the impact (friction, heating, material modifications concerning phase and structure, stratifications, and/or the fibers arrangements, etc.). Simulations by the help of finite element method (FEM) or smoothed-particle hydrodynamics method (SPH) [1] of the impact have become an initial stage in designing new systems, but the experimental validation of models is asked by the particular use of the protective system. The tests on ballistic systems or panels are strictly necessary for evaluating the impact level and for identifying factors influencing penetration and failure mechanisms that could help improve the already existing systems.

Starting from these considerations, the main goal of the study "Ballistic testing of armor panels based on aramid fibers" is the concern of balancing innovations of destructive systems (projectiles, fragments, bullets, etc.) with those that are designated to protect personnel and equipment, using materials like fabrics, woven or multidirectional, stratified and complex composites. At a low speed, even glass fiber fabrics could have satisfactory results [1], but for protecting personnel and equipment at a higher impact velocity, aramid and ultrahigh density polyethylene fibers are more efficient (**Figure 1**) [1, 2].

Even if simulation and modeling offer results closer to the actual processes by using new principles and performance codes and computers in solving impact issues, the experimental work is the final and main stage for the approval of new and improved protective systems. In terminal ballistics, experimental complex techniques, specific equipment, and a testing methodology are required to determine the performance of both the projectile and the protection system and, ultimately, by analyzing the results, to characterize and improve the
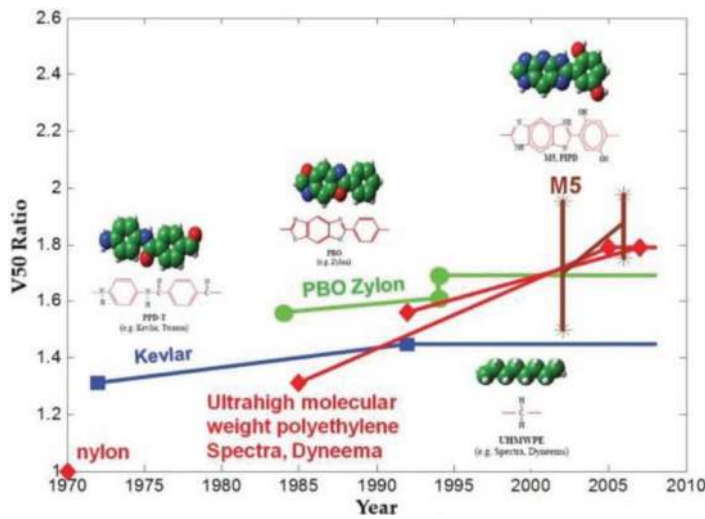

Figure 1. An increase in ballistic performance as a function of the fiber type used in manufacturing body armor [1].

protection system. If, in a classic war, the splinters and fragments are the most dangerous, in other conflicts, bullets remain a major threat to lives and physical integrity of fighters and civilians, representing the main cause of human loss, including during peacetime.

Bullets differ in caliber, initial velocity, mass, jacket, core and shape, and so on. A bullet must have a considerable kinetic energy when reaching the target to penetrate it. In terms of terminal ballistics, mechanical work involves many aspects of bullet-target interaction. Part of the energy is transformed into heat, a part is lost by friction, and the other part by rotating the bullet, by elastic and plastic deformation of both bullet and target. It is a practical impossibility to produce individual ballistic protection equipment that provides total security for the whole arsenal, given the drastic constraint imposed by the limitation of the total mass of protective equipment that a combatant or a user can wear.

In order to assess the impact resistance of protective panels, there are reference standards that offer test methods and procedure, as found in [3]. The test results give the possibility of including ballistic panels in a level of protection. For individual armor front panels, the standards require the absence of perforation for a determined number of repetitions under the same firing conditions, plus a condition related to the depth of the trace generated in a support material (ballistic clays) after impact [4].

The purpose of this chapter includes the process of manufacturing specific flexible ballistic panels made of quatro-axial fiber fabrics in layered composites, tested at fire with 9-mm bullet and 400 m/s (II and IIA protection levels, according to [4]), followed by an investigation of processes and stages of deterioration using scanning electron microscopy (SEM) and macro-photography of the failed zones of the panels after the bullet recovery. Also, a statistical analysis of the depth in the support material [backface signature (BFS)] is presented.

2. Manufacturing and testing the flexible panels

Personnel armor for ballistic protection includes both body systems and helmets. The threats for which this armor is designed are small-caliber projectiles, including bullets and fragments. The level of ballistic protection is taken as the total kinetic energy of a single round that the armor can stop [5].

For polymeric, carbon, ceramic, and glass fibers, researchers reported that the tensile strength increases with decreasing their diameter. For polymeric fibers (**Table 1**), diameters are in the range of 10–15 μm, greater than those for carbon fibers (4–10 μm), but smaller than fibers obtained by chemical vapor deposition, such as boron fibers (100–150 μm). The probability of defects decreases with decreasing the fiber diameter.

Fabrics from fibers and yarns by weaving allow for designing panels that can face both ballistic and blast events. Most ballistic fabrics have two-dimensional plain weave yarns in two orthogonal directions, although some work is being done on three-dimensional weaves and on nonwoven and knitted fabrics [6, 7]. Polymers, glass, and ceramic fibers have high stiffness and high strength-to-weight ratios. From less a decade, the unidirectional and multidirectional

Polymeric fibers	Density (g/cm³)	Modulus (GPa)	Tensile strength (GPa)	Compressive strength (GPa)	Strain-to-failure (%)
Nylon 66	1.14	4.3			25
Silk	1.36	30–60	1.1–2.9		7–12
Kevlar 49	1.45	12.5	3.5	0.4	2.6–4.2
Kevlar 149	1.47	18.5	3.4	0.4	
Kevlar 1000		8.9	2.4–3.4	0.4	2.8–3
Zylon HM	1.56	27	5.8	0.3	2.5
M5 (PIPD)	1.70	27	> 4		>1.4
Vectran	1.47	65	2.9		3.3

Table 1. Typical properties of fibers [2].

fabrics made of polymeric and glass fibers tend to replace the woven ones for certain applications, including panels for the ballistic protection of personnel and equipment.

Figure 2 and **Table 2** present characteristics of threats, as classified by NIJ Standard-0101.06.2008, Ballistic Resistance of Body Armor, and it is obvious that the kinetic energy is the key parameter that will destroy a body armor, for each level of protection.

Many parameters influence the response of fabrics to ballistic impact. These include material properties of and yarn, fabric architecture, boundary conditions, inter-yarn friction, friction between the projectile and the yarn, projectile geometry and velocity, impact direction, and environmental conditions.

The designers of body armor take into account the specific threat that has to face the vest and the helmet. Depending on these threats, the protective body system could be made of polymeric, metallic, and/or ceramic materials, and engineers have to select them. Vests made of
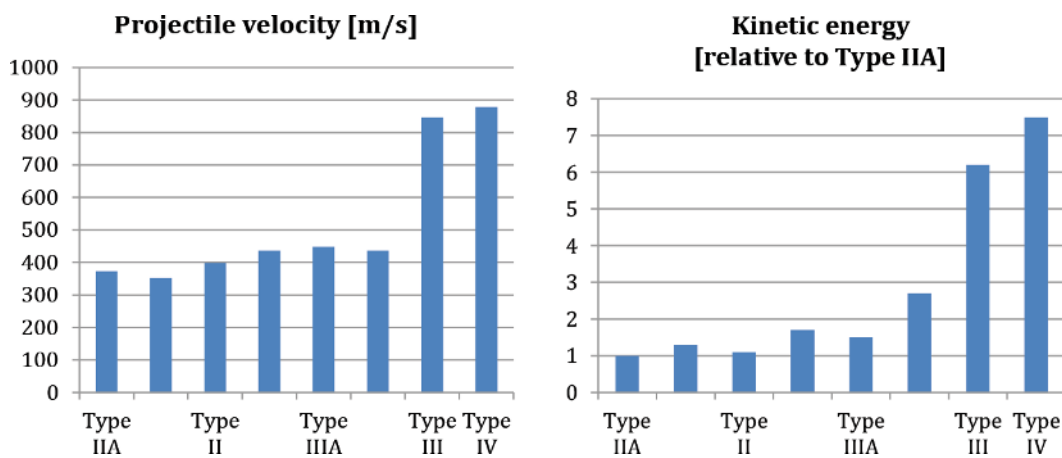

Figure 2. Characteristics of threats as given by NIJ Standard-0101.06. 2008.

Level	Projectile
II	9 mm full-metal-jacketed round nose (FMJ RN) 0.40 S&W FMJ
IIA	9 mm FMJ RN 0.357 magnum-jacketed soft point(JSP)
III	0.357 SIG FMJ flat nose (FN) 0.44 magnum semi-jacketed hollow point (SJHP)
IIIA	7.62 mm FMJ, steel-jacketed bullets (U.S. military designation M80)
IV	0.30 caliber armor piercing (AP) bullets (U.S. military designation M2 AP)

Table 2. Levels of ballistic resistance [5].

only polymeric materials are intended for protecting human body against fragments and lower velocity projectiles. Glass fibers and polyamide fibers were firstly used, but polyaramid fibers, introduced by DuPont [8] and later by Teijin [9], make the armor lighter and more reliable for a greater ballistic limit V_{50}. In the 1980s, fibers made of high-molecular-weight polyethylene (UHDWPE) and polybenzobisoxazole (PBO) have also been used.

Body armors have to fulfill two types of requirements:

- to arrest (stop) the projectile within the armor, even to withstand multiple hits on the same armor panel, depending on the protection level the armor is classified in; and

- to have a deflection that would not severely injure the wearer.

There is no universal method to design an armor system, but the report "Opportunities in Protection Materials Science and Technology for Future Army Applications" [10] gives a flow chart of activities for homologating a new or a redesigned armor, pointing out the place and importance of simulation based on the actual material properties when bearing a high strain rate as in ballistic impact (**Figure 3**). Certainly, the main stage in evaluating the armor is the shoot test.

New materials are developed, but these are infrequently selected for protective systems because their behavior in actual events and configurations is not directly related to the laboratory tests. Moreover, most non-armor application materials are chosen according to their bulk quasi-static properties, even though such properties do not always predict their ballistic performance. If the constitutive relations for properties characterizing new materials needed for running simulations are not known, then the engineer has to use information from the most similar existing material [11], making the result uncertain. This is another reason why armor designers do not consider using new-entry materials that have not yet been sufficiently characterized under particular dynamic conditions. The simulation is often done as a guide to identify trends due to design modifications than as a source of practical results. The modeling of a protective system or a panel is difficult to do at different levels [12, 13]. For instance, the panel made of polymeric fibers of an armor could be considered as a stratified material at macro-level (**Figure 4**), but each layer is a fabric, woven or unidirectional, that contains yarns, their cross-dimensions being thousand times smaller than their length. This could be a
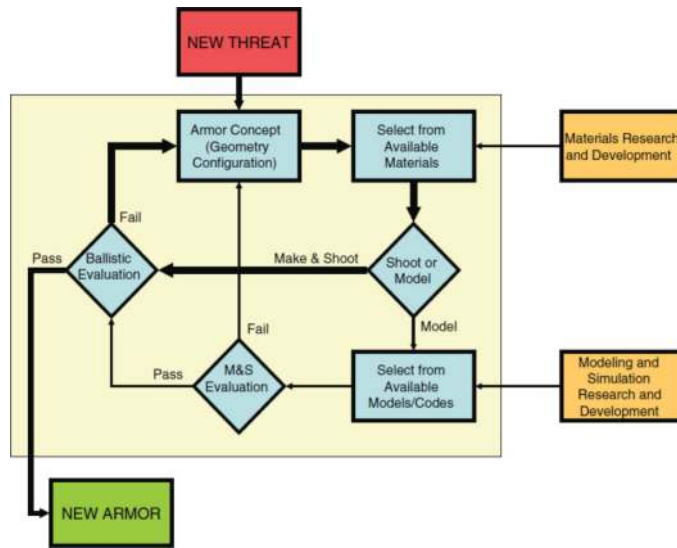
Figure 3. Flow chart of new or redesigned armor [10].

mezzo-level in modeling [14]. And there is the micro-level: each yarn contains hundreds of fibers, their diameter also being smaller by several orders of magnitude. The simulation could not cover all these levels at the same time, in one model, and the designers have to rely on their experience and ingenuity to generate a model that could help restraining the feasible solutions.

The panels were made of layers of Twaron LFT SB1plus, as supplied by Teijin Aramid [9], a new entry on the market in 2012. The four sublayers of LFT SB1plus, laminated together with a very thin sheet of resin, are visible as shown in **Figure 5**: the angle positioning of the

a) 8 layers (t=10⁻⁴ s), 7 broken layers   b) 12 layers (t=10⁻⁴ s), 4 broken layers
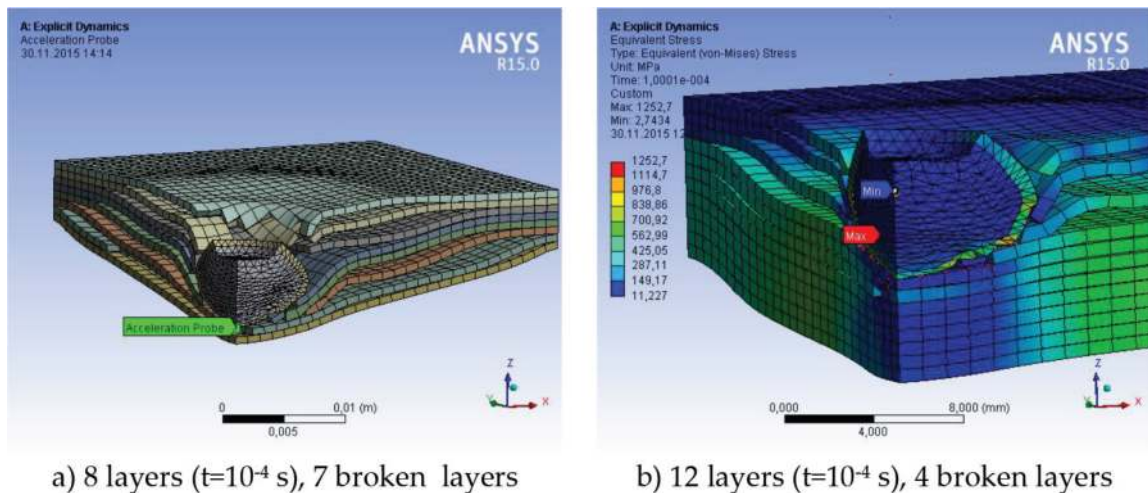
Figure 4. A simplified isothermal macro-model of a flexible panel (v = 400 m/s, friction contact between bodies: Friction coefficient between layers 0,4, friction coefficient between layers and bullet: 0.3 [14], bilinear hardening constitutive models for materials) (see **Table 3**). (a) 8 layers (t = 10^{-4} s), 7 broken layers. (b) 12 layers (t = 10^{-4} s), 4 broken layers.

unidirectional yarns of sublayers being 0, 90, 45, and −45° and the specific area density 430 g/m². The layers in a panel were secured by sewing on two edges to maintain the integrity and order of the layers. The sewing line had a length of approx. 200 mm, made at 25 mm from the panel edge, with a step of 2–2.5 mm.

The manufacturing of the panels consists of cutting squared layers of 500 × 500 mm, having an area of 0.25 m², from fabrics with the width of 1200 mm. The area value positioned these panels between NIJ-C-4 (0.23 m²) and NIJ-C-5 (0.3 m²) for large and very large surfaces. After cutting the squared layers, these were arranged in three types of panels, each one containing a different number of layers: 4, 8, and 12, respectively (**Table 4**). The number of layers was selected after a simulation [14] at macro-level (**Figure 4**), with layer properties similar to aramid fiber, as given in the study [15].

Taking into account the standard Ballistic Resistance of Body Armor, NIJ Standard-0101.06, U.S., 2008, the test plan for flexible ballistic protection panels based on aramid fibers included the fire with 9-mm bullet for level II and level IIA (**Figure 6**).
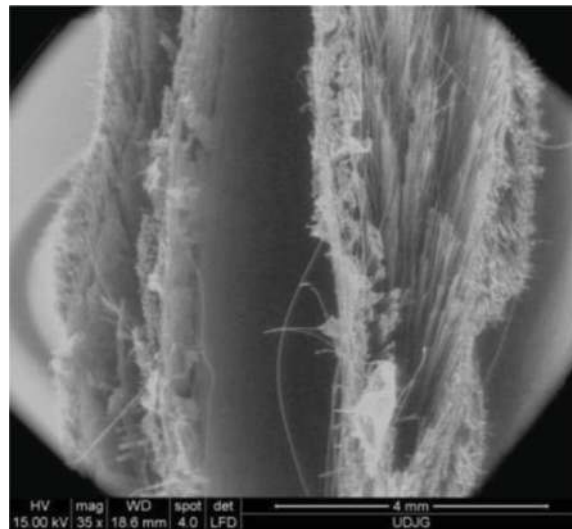

Figure 5. Cross section on a LFT SB1plus fabric (4 sublayers (0, 90, 45, −45), each one with unidirectional yarns).

Material	Young modulus, Pa	Poisson coefficient	Bulk modulus, Pa	Shear modulus, Pa	Yield limit, Pa	Tangent modulus, Pa	Max. equivalent plastic strain, EPS
Layer	7×10^{10}	0.35	7.77×10^{10}	2.59×10^{10}	6.3×10^{8}	1.9×10^{10}	0.06
Copper alloy (bullet jacket)	1.1×10^{11}	0.34	1.14×10^{11}	4.10×10^{10}	2.8×10^{8}	1.15×10^{9}	—
Lead alloy (bullet core)	1.6×10^{10}	0.44	4.44×10^{10}	5.55×10^{9}	3×10^{7}	1.1×10^{8}	—

Table 3. Material properties for the impact model bullet—Stratified pack [11].

Panel	Number of layers	Calculated mass (g)
LFT SB1 plus	4	450
	8	900
	12	1300

Table 4. Calculated mass of a flexible panel.

In order to evaluate the impact resistance of the protective panels, there are reference standards proposing testing methods, the results being ranked as a protection level, characterized especially by the projectile mass and velocity. For panels used as body armor, these standards require the absence of total perforation and a supplementary condition of limiting the back deformation as human body could not face a high deformation without critical injuries, even fatal, even if the bullet does not penetrate this one. As testing directly on the human body is not recommended neither ethical, panels are required to have a maximum value in a support material that could be similar (in a closer manner) to the human body response, as, for instance, the ballistic clay.

The impact velocity (just before hitting the target) was measured with the help of a system including a chronograph Oehler model 43, stable for the temperature range of 5–40°C and having an accuracy of 0.3%. Other measurement devices used for these tests were a ballistic barrel for bullets of 9-mm FMJ (fulfilling the requirements of NIJ 0101.04/2000) and a fire arm table with a blow-back compensation [4], a hygrometer with an accuracy of 1%, a barometer with an accuracy of 1 mm Hg, a thermometer with an accuracy of 1°C, a box for the ballistic clay, an oven allowing for tempering at 20 ± 5°C, a climate enclosure allowing for maintaining a temperature of 20 ± 5°C, and an oven for ammunition conditioning. A partial view of the test facilities is presented in **Figure 7**.

The shooting was done in the Scientific Research Center for CBRN Defense and Ecology laboratory, by specialized personnel in order to fulfill the requirements of reference [4], including the arrangement shown in **Figure 8**, the distance between fires and the distance from

Figure 6. Tested panel made of 12 layers of LFT SB1plus.

Figure 7. Fire laboratory at the scientific research center for CBRN defense and ecology, Bucharest, Romania.

the panel edges and the regulations of protection, specific to this type of laboratory, being observed [16].

The framed box has the dimensions $610 \times 610 \times 140$ mm (± 2 mm). The back of the box is detachable, and it was made of wood (19.1 mm). The frame is made of steel and helps the ballistic clay to be leveled. As recommended by [4, 5], the clay grade was Roma Plastilina no. 1, which has a durability of about 1 year. This clay must have no voids, a smooth-free surface, and it has be easy to level with a ruler, the free surface being determined by the metal frame.

The panel behavior was evaluated by the number of failed (broken) layers and by the values of backface signature (BFS). **Figure 9** presents the method of measuring the depth of the impact deformation within the support material.

The determination of ballistic resistance of protection materials and equipment at the action of infantry bullets is carried out according to NIJ Standard-0101.06 [4] (**Figure 6** presents one of the tested panels). The samples were tested with a ballistic pipe (with a measured velocity of
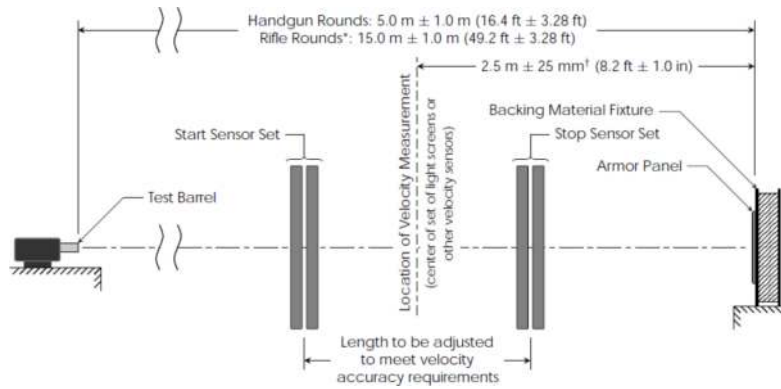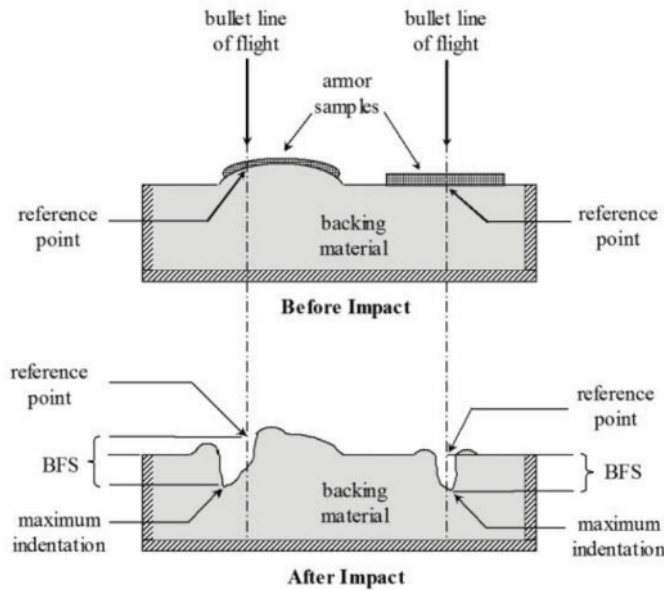
Figure 8. Shooting arrangement [4].

Figure 9. Measuring the BFS according to ballistic resistance of body armor, NIJ Standard-0101.06, U.S., 2008 [4].

430 ± 10 m/s), with a projectile of 9-mm full metal jacket (FMJ) bullet. The deformation remained in the ballistic clay (backface signature or BFS) that was measured according to [4], with a depth caliper, with an accuracy of ±0.1 mm. After each measurement, the calipers were cleaned to avoid any traces of clay on the measuring area. The evaluation of the total penetration of a package is in many cases simple, when a hole with a diameter at least equal to the size of the bullet is found and the entire bullet passes through it. When testing individual ballistic protection equipment, the trauma to the human body is evaluated by the depth of the print that is formed in the clay on which the sample is fixed.

Environmental parameters inside the fire enclosure were as follows: temperature: 20°C (±5°C), relative humidity: 50–70%, atmospheric pressure: 760 mm Hg (±15 mm Hg).

After the fire, the projectile or their fragments were removed from the clay. The clay was added anytime needed, after measuring the backface signature (BFS).

The fire procedure has the following steps:

- the test equipment is positioned in the mounting bracket at the distance required for each equipment from the muzzle; the types of armaments and ammunition required by each level of protection for which the test is being conducted, for Level II and IIA [4] in this study;

- positioning the bullet speed measurement system, starting at a distance of 2 m from the muzzle, so that the frames of the system are in planes perpendicular to the fire direction; the distance between the frames is set at 0.5 m; distance measurements are made with an accuracy of 1 mm;

- fire runs on the sample panel.

3. Evaluation of ballistic resistance for the flexible panels made of aramid fibers

At molecular level, variables in polymers include chemical makeup, the length and degree of branching of molecular chains, the degree of alignment and entanglement, and the extent of cross-linking. The types and strengths of bonds in chains and among chains influence the polymeric fiber strength and strain and influence the failure mechanisms.

The factors affecting the ballistic performance may be grouped into three categories:

- the factors of projectile (mass, velocity, materials, shape, and impact direction);

- the target architecture (material, structure at nano-, micro-, and macro-level); and

- the environment (temperature, humidity, clamping, and support material as, for instance, the human body or the car body).

When fabrics are impacted by a projectile, the target size, its clamping conditions are important. A longer yarn can absorb more deformation energy than a shorter one before failure. Thus, a larger target area will lead to a higher energy dissipation. However, this is not true when the velocity of the projectile is very high as compared to the velocity of the shock wave in the fibers since only a small zone of the target can dissipate the kinetic energy of the projectile. The boundary conditions of the target also play an important role. Shockey et al. [17] observed that a two-edge gripped fabric absorbs more energy than a four-edge gripped fabric, and fabrics with free boundaries absorb the least energy. Chitrangad et al. [18] observed that when pretension is applied on aramid fabrics, their ballistic performance is improved. Zeng et al. [19] observed that for four-edge gripped fabrics, energy absorbed is improved if the yarns are oriented at 45° relative to the edge.

The number of fabric plies or sublayers also affects the ballistic performance (note that typically there may be 20–50 plies). Shockey et al. [17] observed an increased specific energy absorbed for multi-ply targets due to friction forces between layers. The influence of interplay materials and the distance on ballistic performance have also been investigated [7]. The influence of a projectile geometry also becomes less important with an increased number of plies [20].

Frictional effects between a projectile and a fabric are observed at a low-velocity impact, but they diminish at a higher velocity [17]. Friction does help maintain the integrity of fabrics in the impact region by allowing more yarns to be involved in the impact and it increases energy absorption by increasing yarn strain and kinetic energy. Dischler [21] applied a thin polymeric film on Kevlar (20-ply), which increased the coefficient of friction from 0.19 to 0.27 and reported a 19% improvement in ballistic performance in stopping a flechette. Carrillo et al. [22] investigated the ballistic behavior of a multilayer Kevlar aramid fabric/polypropylene (atactic PP films of 0.032 mm and a density of 910 kg/m^3) composite laminate and simply plain-layered aramid panel (plain-woven Hexcel aramid 720 fabric, Kevlar129 fiber, 1420 denier), under a sphere impact (with a diameter of 6.7 mm and a mass m of 1.11 g), at a velocity of 274.5 m/s and found that the improved performance of composite laminate is due to the fact that the thermoplastic matrix enables energy-absorbing mechanisms, such as fabric/matrix debonding and delamination.

There is a tendency to combine high-resistance fabrics with lower cost ones, but the results are still indecisive. Yahaya et al. [28] presented ballistic properties of non-woven kenaf fibers/Kevlar epoxy-hybrid laminates with thicknesses ranging from 3.1 to 10.8 mm, when impacting with a 9-mm full metal jacket bullet at speeds varying from 172 to 339 m/s, at normal incidence, but hybrid composites recorded a lower ballistic limit (V_{50}) and energy absorption than the Kevlar/epoxy composite.

The processes evidenced by macrophotography and SEM images help for understanding the failure mechanisms specific for the designed panels with layers of LFT SB1 plus a quatro-axial fabric.

Taking into account reference works [23], several stages for this type of panels were identified:

Stage I is dominated by deformation, yarn breakage, and energy dissipation mechanisms; the moment transfer between the projectile and the fabric leads to an increase in the kinetic energy of the fabric, which initially leads to the production of the pyramidal deformation, less evident on flexible panel with unidirectional fibers (see **Figure 10** with photographs 1F-1 and 2F-1). Simultaneously, the yarns begin to stretch as the longitudinal wave propagates along the thread, leading to an increase in internal energy and/or wire deformation (statistical process). The sheet of resin, even very thin, keeps the yarns in positions, being more difficult to be laterally impelled.

Stage II is characterized by friction produced by pulling the yarns; one or more yarns can be pulled out of the fabric and a large amount of energy dissipates through this sliding friction; the rate of deceleration is lower at this step than in Stage I, but excessive yarn drawing promotes the fabric opening mechanism, the bullet pushing several yarns laterally. The fabric pattern or the way of arranging and maintaining the unidirectional yarn compaction (by sewing or a rare weaving with other types of fibers that maintain the surface density of yarns) influences the opening mechanism.
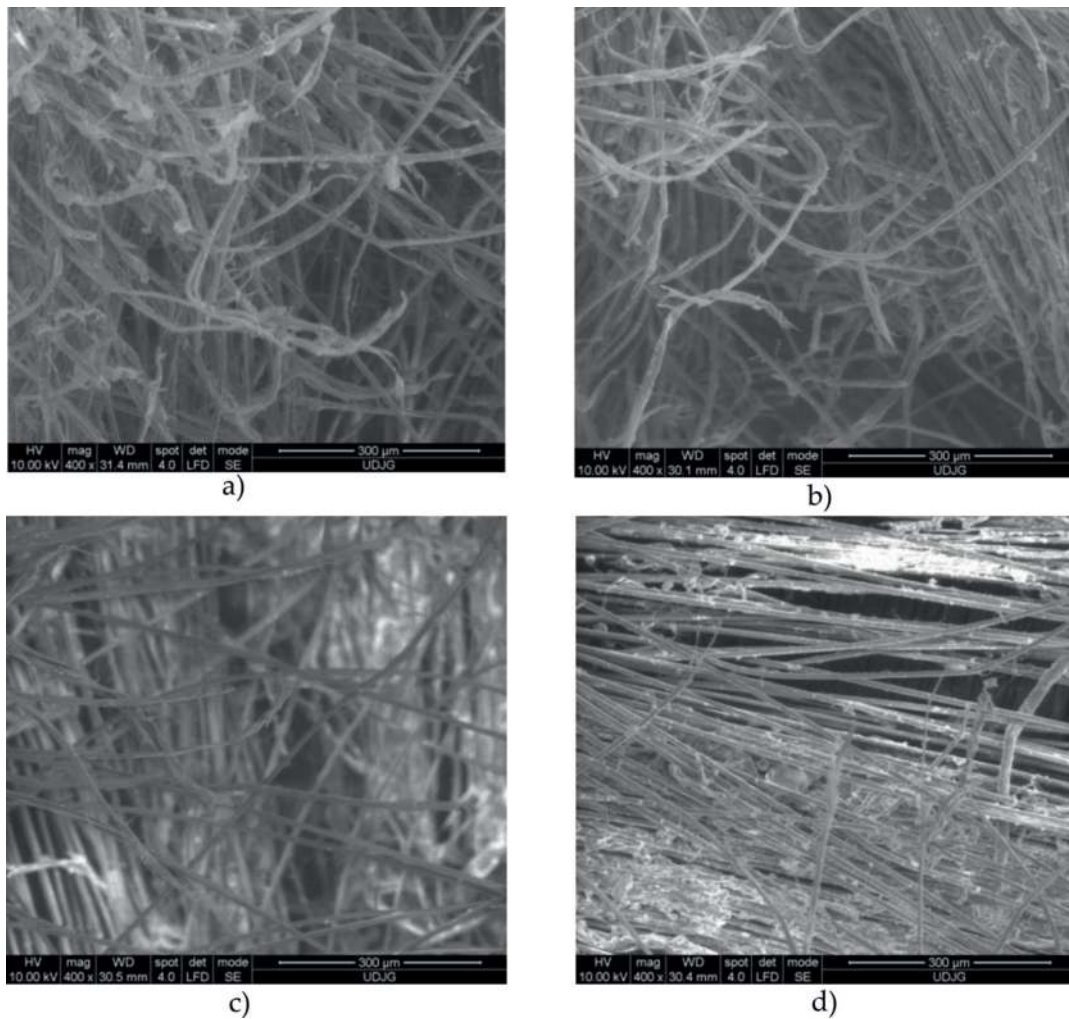
Figure 10. Posttest images of fabric damage from a panel made of a layer of LFT SB1plus, showing yarn and fibers' breakage characteristics. (a) 1F-1. (b) 2F-1. (c) Fiber damage on the front of 3-rd layers (3F-1). (d) Fiber damage on the back of the 12-th layer of a panel (12B-1).

Stage III corresponds to the postimpact region for impact without penetration, and the projectile can be arrested in the fabric. The bullet is strongly flattened, remaining with the typical aspect of mushroom (see **Figure 15**). Depending on material, projectile, and impact parameters, these steps may differ in duration and appearance.

4. Failure mechanisms of panels, yarns, and fibers by SEM and macrophotography investigations

The study of ballistic impact of fabrics includes residual velocity, stroke response, energy absorption, and tensile properties of yarns and failure mechanisms [17].

Mechanisms of energy dissipation are breaking the fibers/yarns, fibers' deformation (stretching, twisting) (see **Figures 11a** and **16c**), fiber fibrillations (**Figures 12** and **16c**), bullet deformation and cracking, local heating, acoustic energy, air entrainment, cross-sectional deformation of yarn (**Figure 16b**) and friction among yarn fibers, yarns, and also friction between these ones and the bullet.

Types of damage in filaments, yarns, and fabrics may be noticed at both micro- and macro-levels. The micro-level involves breaking bonds that are involved in the structure of the
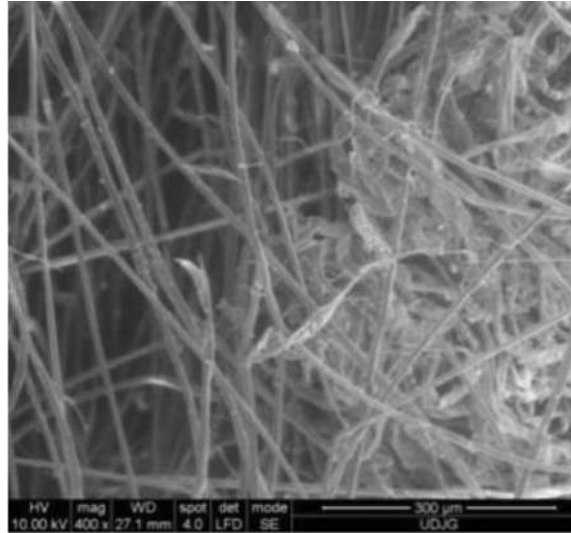

Figure 11. Fiber break in the third layer of the panel (front view, code 3F-1); less fibers with fibrillation.
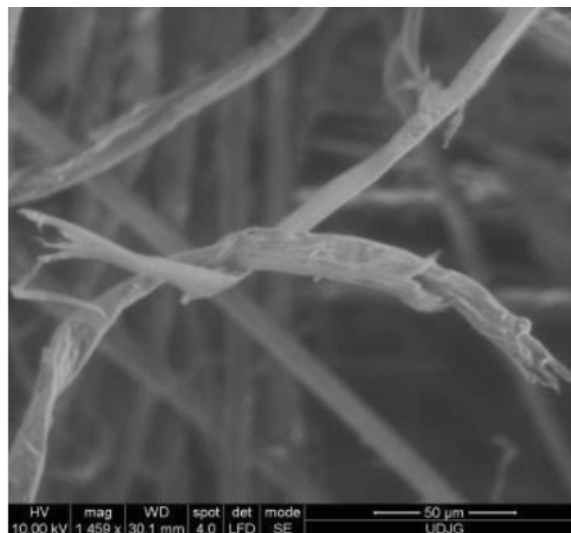

Figure 12. Fibrillation of fibers (front view, code 2F-1).

filaments, while at the macro-level, the destruction may be characterized by mechanisms such as yarn pulling or bowing.

Higher magnifications show that the fibrils in broken fibers are also stretched (see **Figure 10b**). Fiber material very likely has plastic strain but, more obviously, localized plastic ones, failure also occurring due to nucleation of voids, cracks, and shear bands. Failure initiators are thought to originate in material defects such as tiny voids, foreign particles, and chain entanglements, resulting from chemical non-homogeneities or manufacturing procedures.

Fiber failure modes other than tensile failure are also observed. The influence of the structure of polymeric fibers at nano (molecular)-level on failure behavior is not well understood, especially at high strain rates and high pressures [3].

When a projectile hits a fabric or a panel made of layers of fabrics, it is caught by the yarn network (woven or not). Kinetic energy is transferred to the fabric as the stress wave spreads outward from the point of impact. The energy is partially dissipated by fiber deformation and breakage and by friction caused by inter-fiber slippage. A projectile with a sufficiently high mass and velocity may penetrate the fabric and cause it to fail.

Figure 10 indicates that tensile fracture first occurred at defects such as voids and kinks and was assisted by the residual stresses that are induced during processing. Similar mechanisms were reported by Allen et al. [24].

For example, a projectile impact on fabric compresses the fabric against the backing layers and causes transverse loads on the yarns and fibers that can result in deformation and failure (breakage). When compressed fibers are examined by SEM, they and the fibrils show flattening, kinking, and buckling (see **Figures 11** and **16c**).

When a projectile hits the individual fiber or a yarn [14, 16], longitudinal and transverse waves propagate from the impact point. Most of the kinetic energy transfers from the projectile to the principal yarns (those that come directly into contact with the projectile). The orthogonal yarns, which intersect the principal yarns, absorb less energy. The transient deformation within the fabric was simulated by Grujicic et al. [12]. The transverse deflection continuously increases until it reaches the breaking strain of the fibers and causes failure. Failure mechanisms characterizing the fabrics under ballistic impact include

- breakage of fiber bonds and yarns,

- yarn pullout,

- remote yarn failure,

- wedge-through phenomenon (hole smaller than the diameter of projectile),

- fibrillation,

- effects induced by friction between the projectile and the fabric, yarn, and fibers.

In accordance with the kinetic theory of rupture, breaking the bond occurs when it is excited beyond its activating energy. When activation energy or stress for a particular type of destruction is reached, the failure mechanism is triggered.

Localized fracture of the yarn occurs when all fibers of the yarn break almost in the same location, usually at the sharpest point of a penetrator. This type of failure is accompanied by a popping sound and a sudden decrease in the measured load. The two causes of yarn breakage are the traction of yarns along their length and the shear in their thickness. The fiber in this yarn will break when the induced strain exceeds the strain at breakage that depends also on the strain rate but the strain at breakage generally decreases as the strain rate increases.

The breakage of yarns could occur at different points along their length and not necessarily at the point of impact. Also, if the penetrator is not too sharp, it compresses the superficial material between its front and the bulk material, outside its contact to the target, and the yarns could be pulled up and could break in traction.

In multilayered (stratified) systems, **friction** between layers is important in reducing damage [11]. All projectiles penetrating through a fabric, with semispherical, ogival, or conical shape, cause a splitting of the yarns [25]. Martinez et al. [26] have stipulated that pulling or rubbing is involved during the fabric-woven manufacturing and that its severity depends on the contact pressure between the layers.

The yarn pulling occurs when none of the yarn fibers break, but the yarn is pulled out of the fabric mesh. This type of failure can happen to lose or unfixed yarns (on the edge). The force required to pull the yarn from the net depends on the frictional force on the contact area between the yarn in question and the other perpendicular yarns with which it intersects (for woven fabrics) or on the friction among yarns and sublayers when the fabric is made of unidirectional yarns. As the yarn is pulled out, the number of yarns intersecting constantly decreases, resulting in a gradual decrease in the measured impact load.

Splitting of fibers along their length or fibrillation is a type of destruction favored by the abrasive action on the fiber length (but also uneven traction along the fiber and their local defects play an important role in fibrillation).

The bowing is dominant in the back layers of a multilayer panel, where the projectile attempts to penetrate through a tip-edge approach, after that, it is considerably slowed down by the back layers that did not fail. The passing process of the projectile through the layers usually produces a hole less than the diameter of the projectile in the first layers, a smaller number of yarns being broken as compared to the number of threads intersecting or contacting the projectile [27]. Typical aspects of the aramid fiber failure are given in **Figures 12** and **13**: micro-fibrillation, peeling, and shear, but also fiber twisting and thinning zones along the fiber. An obvious less strain rate could be noticed in **Figure 13** as compared to that in **Figure 12**.

A study at the macro- and micro-level was done for pointing out the failure processes characterizing each layer. **Figure 14** shows the front and back views of the panel made of 12 layers LFT SB1plus. On this type of package, a partial penetration was obtained, that is, the destruction of the first four layers of the panels. The photographs show the entire pack after testing with three shots. It is obvious from **Figure 14** that the design of the unidirectional fabrics helps yarns to develop a better resistance against pulling out.
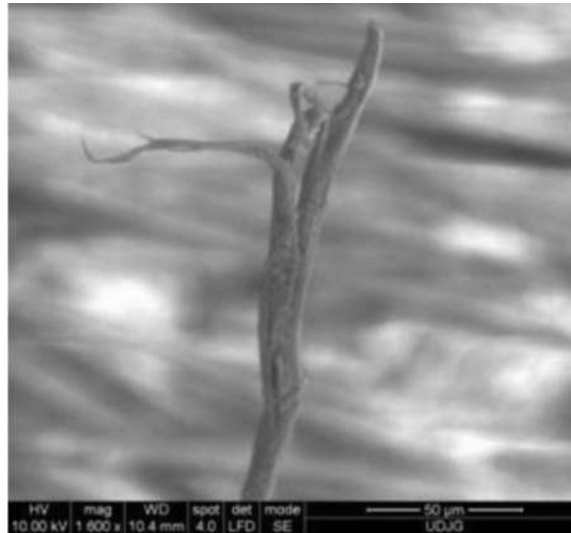
Figure 13. A fiber broken on the back of the last layer (the 12th layer).

The layers may be grouped as follows (**Figure 14**):

• layers with hole dimensions less than the projectile diameter (layers 1 and 2 from the studied panel),

• layers laterally impelled (pushed) (layers 3 and 4),

• layers only compressed, with a shallow print of the arrested bullet (layers 5–11),

the last layer with pull-out yarns and disorder yarns, especially on the back of the last layer (layer 12).

An investigation of the arrested bullet offers details on how the yarns are broken. **Figure 15** shows that the projectile attack makes the yarn to break laterally from the direct impact, mainly from tensile solicitation. On the top of the projectile, the fragment of the yarn remains. One may notice an orientation similar but not exactly as the orientation of yarns in the four sublayers (0, 90, 45, −45), meaning the bullet is forced to change the initial position due to yarn resistance and break unevenly. The jacket of the bullet is split like a flower petal and migrates toward the boundary of the lead core. When the core hits the target, it is strongly compressed and laterally expanded, some of the yarn fragments being embedded into the lead alloy.

The holes in layers 1 and 2 are similar, resulting that the process of yarn destruction is also similar, which argues that the perforation of the first two layers is made approximately with the same parameters (the velocity of the bullet through the first two layers is not significantly reduced and the shape of the bullet is not modified too much because it does not face yet the resistance of the other layers and it only cuts the yarns, as it is presented in a FE model in [11, 14]. It is worth mentioning that the tests were carried out under conditions of a small variations in the initial bullet velocity (410–430 m/s). The impact angle is normal on the target surface, with deviations of less than 5% at the mouth of the pipe.
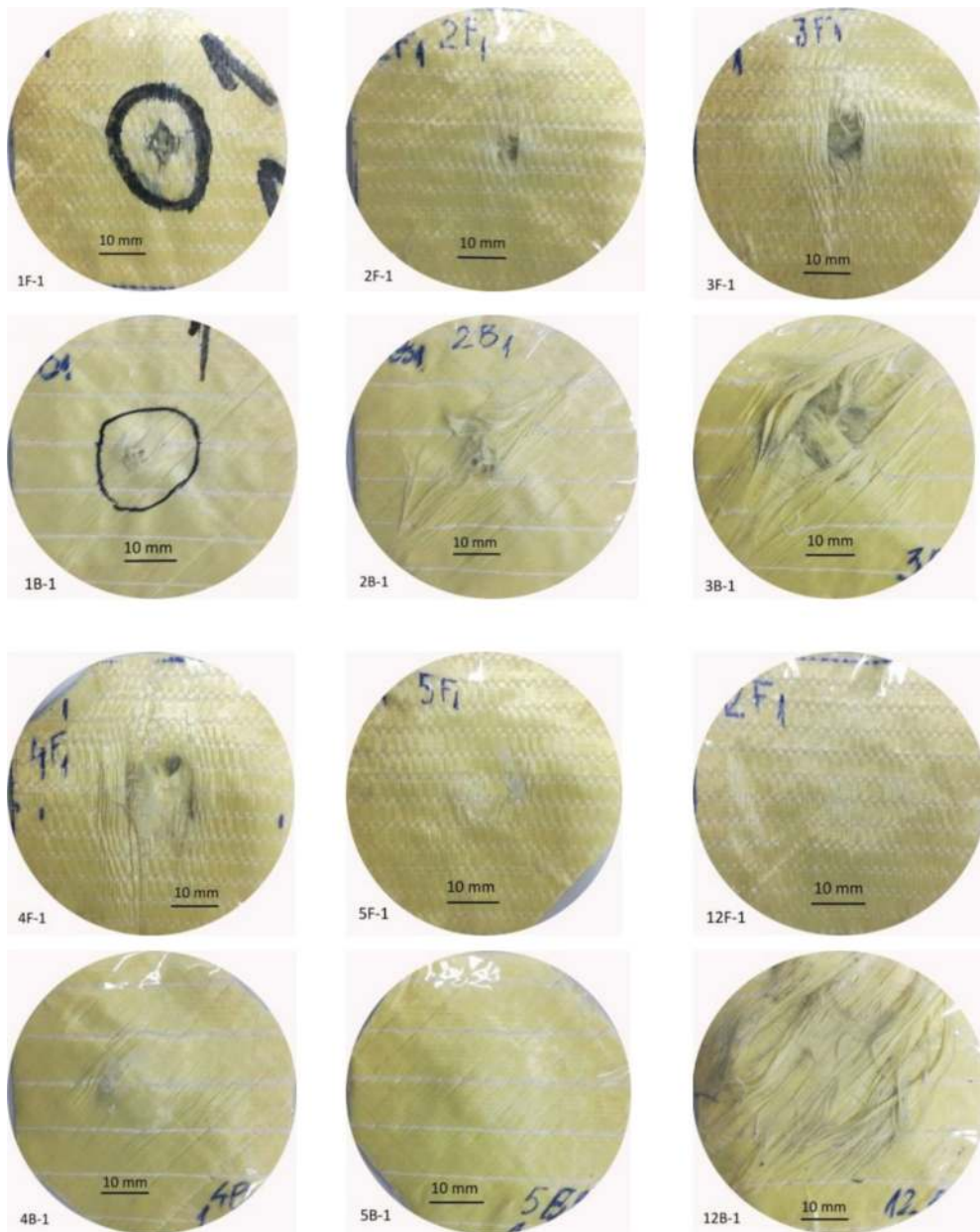
Figure 14. Macrophotographic study of a panel made of 12 layers of LFT SB1plus.

Starting from layers 3 and 4, the widening of holes and the pulling-out process of the yarns are noticed. Layer 4 is the last layer in the LFT SB1plus panels through which bullets have passed or stopped (arrested).

Layer 5 shows more uniformly circular shapes of crushing/compression, imparting a tendency to uniformize the response of the material.

Figure 15. The bullet extracted from the sample panel presented in **Figure 14**. (a) Front view. (b) back view of the same bullet.
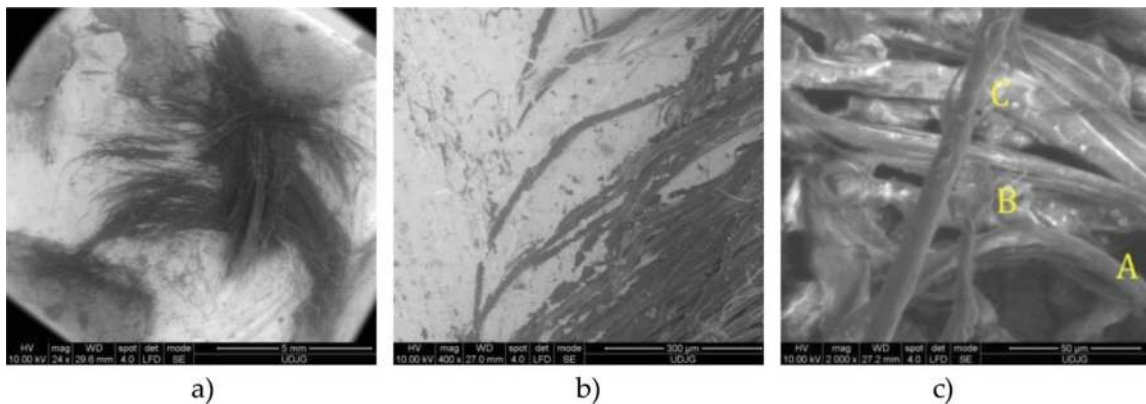

Figure 16. SEM images of the bullet with fragments of yarns on its front. (a) SEM image of the flattened bullet, as extracted between the fourth and the fifth layer. (b) Magnification of embedded fibers, very probably from the first yarn touching the bullet. (c) A—Fibrillation, B—Break by tensile loading with twisting of the fiber end, C—Necking of the fiber without break.

Figure 16a shows the fragmentation of fibers and the embedding of the yarn fragments remained under the bullet, with details shown in **Figure 16b**. **Figure 16c** points out the types of failures on the fibers remained on the projectile.

5. A statistical analysis of backface signature

The values of BFS for panels made of layers LFT SB1plus are given in **Table 5** and they were measured according to Ballistic Resistance of Body Armor, NIJ Standard-0101.06, 2008 [4].

NIJ Standard-0101.06 [4] asks for having fires complying with requirements concerning the shot-to-edge distance and shot-to-shot distance (minimum of 51 mm). For armor types subjected to a single threat and for the lighter weight threat round when two threats are

LFT SB1plus Layers/identification code	Shots		
	1	2	3
	BFS (mm)		
12/8	18	12	23
12/9	16	14	20
12/11	20	24	21
12/12	21	23	21
12/14	17	22	19
8/3	27	TP	
8/5	30	TP	
8/6	31	33	TP
4/1	TP		
4/2	TP		
4/3	TP		

Table 5. BFS for panels made of layers of LFT SB1plus.

specified, the minimum shot-to-edge distance shall not be greater than 51 mm. For the heavier threat round when two threats are specified, the minimum shot-to-edge distance shall not be greater than 76 mm.

Each test panel must withstand the appropriate number of fair hits and may not experience any perforations. Any complete perforation by a fair hit constitutes a failure. Each new size of a body armor model shall either have no BFS depth measurements that exceed 44 mm (**Figure 17**), or for each threat round, an estimated probability of a single BFS depth measurement exceeding 44 mm of less than 20% with a confidence of 95%.

The armor model shall be deemed to meet these requirements if no BFS depth measurement due to a fair hit exceeds 50 mm, and either

- all BFS measurements due to fair hits are 44 mm or less or

- the one-sided tolerance interval for a normal distribution indicates that there is 95% probability that 80% of the test BFS measurements for armor samples of that particular model, size, condition, and test threat will be 44 mm or less.

In this case, the upper tolerance limit, Y_U, and the sample standard deviation, s, of all recorded BFS measurements for body armor sample panels of a particular model, size, condition, and test threat shall be calculated, and

$$Y_U = \overline{Y} + K_1 s \tag{1}$$

where $\overline{Y}$ is the average of all BFS measurements for armor samples of that particular model, size, condition, and test threat; s is the sample standard deviation of the same set of BFS measurements; and K_1 is a factor that must be determined such that the interval covers the appropriate proportion, with a confidence of γ.
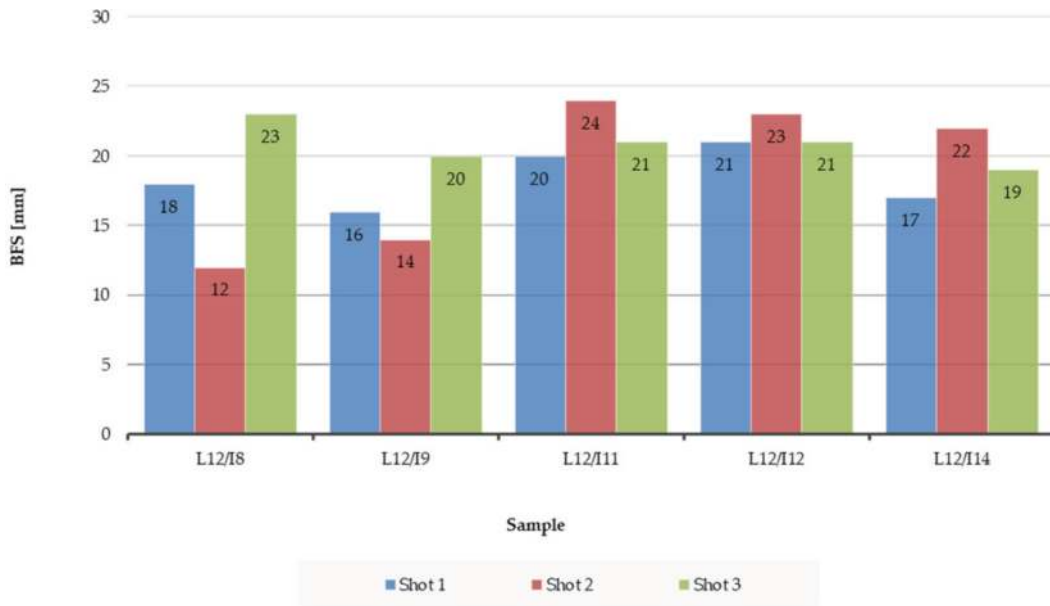
Figure 17. BFS results, based on the number of shoots/panel, for panels made of 12 layers of LFT B1plus.

The average $\overline{Y}$ is simply calculated as

$$\acute{Y} = \frac{1}{N}\sum_{i=l}^{N} Y_i \tag{2}$$

where N is the number of BSF measurements and Yi is the BFS value for the i-th shot. The standard deviation of the sample population, s, is calculated with the relationship:

$$s = \sqrt{\frac{1}{N-1}\sum_{i=1}^{N}\left(Y_i - \acute{Y}\right)^2} \tag{3}$$

The approximate factor, k_1, for a one-sided tolerance interval can be calculated as

$$K_1 = \frac{z_{1-p} + \sqrt{z_{1-p}^2 - ab}}{a} \tag{4}$$

where z_{1-p} is the critical value of the normal distribution which is overpassed with a probability $1 - p$. The factors a and b are defined as

$$a = 1 - \frac{z_{1-\gamma}^2}{2(N-1)} \tag{5}$$

$$b = z_{1-p}^2 - \frac{z_{1-\gamma}^2}{N} \tag{6}$$

where z_{1-p} is the critical normal distribution which is overpassed by a probability $1 - \gamma$.

In order to analyze the BFS measurements in accordance with [4], the probability for no BFS measurement to be higher than 44 mm has to be at least 80%, thus $p = 0.80$ and the confidence coefficient is 95%

$$\gamma = 0.95 \tag{7}$$

The critical values for the normal distribution for this case study are

$$z_{1-\gamma} = z_{0.05} = 1.645$$

$$z_{1-p} = z_{0.20} = 0.842$$

Using these data, the factors a and b may be calculated for an imposed number of BFS measurements, N. For N = 15, the factors a and b are

$$a = 1 - \frac{1.645^2}{2(15-1)} = 0.903, \qquad b = 0.842^2 - \frac{1.645^2}{15} = 0.528.$$

And the factor k_1 is

$$k_1 = \frac{0.842 + \sqrt{0.842^2 - 0.903 \cdot 0.528}}{0.903} \approx 1.466$$

The allowable excessive BFS probability, 20%, may appear to be high; however, this value is intended to account for both the variation in the armor's performance, which should be small, and the variation in the BFS measurement due to the backing material and the backing material preparation. While careful treatment and preparation of the backing material by the test laboratory can minimize the variation due to the backing material, there will always be some inherent variation introduced into the test results by the backing material. The required probability is chosen to reduce that possibility that an acceptable armor design will fail the PBFS test due to reasonable variation in the backing clay.

The average value of BFS $\acute{Y}$ was calculated for panels made of 12 layers of LFT SB1plus, with N = 15 (the values of BFS are given in **Table 5**)

$$\acute{Y} = \frac{1}{N} \sum_{i=l}^{N} Y_i = 19.4 \ mm$$

where N is the number of measured BFSs and Y_i is the value of measurement i for BFS.

The standard deviation of the sample population, s, for panels made of 12 layers LFT SB1 plus is equal to

$$s = \sqrt{\frac{1}{N-1} \sum_{i=1}^{N} \left(Y_i - \acute{Y} \right)^2} = 3.439$$

The upper tolerance limit, Y_u, for panels made of 12 layers LFT SB1plus is

$$Y_u = \acute{Y} + k_1 s = 19.4 + 1.466 \cdot 3.439 = 24.441 \; mm$$

6. Conclusions

This chapter underlines the necessity of testing ballistic protection packs made of LFT SB1 plus against a certain threat in order to assess their resistance to this specific threat and the investigation of failure mechanisms in order to improve their behavior at ballistic impact.

Ballistic testing of the LFT SB1 plus panels can provide reliable information about the new material.

Tests made on packs made of LFT SB1 plus according to NIJ Standard-0101.06-2008 gave good results for the packs made of 12 layers of this fabric and the BFS was measured.

The upper tolerance limit of 24,441 mm obtained for backface signature recommends this panel of 12 layers of LFT SB1 plus for protection level of IIA, according to the abovementioned standard.

Author details

Catalin Pirvu[1]* and Lorena Deleanu[2]

*Address all correspondence to: pirvu.catalin@incas.ro

1 National Institute for Aerospace Research "Elie Carafoli"—INCAS, Bucharest, Romania

2 Department of Mechanical Engineering, "Dunarea de Jos" University of Galati, Galati, Romania,

References

[1] Năstăsescu V, Ştefan A, Lupoiu C. Analiza neliniară prin metoda elementelor finite. Fundamente teoretice şi aplicaţii. Academia Tehnică Militară Bucureşti. 2001

[2] Cunniff P. Fiber Research for Soldier Protection. U.S. Army Natick Soldier Research. Development and Engineering Center; 2010

[3] Hinton MJ, Kaddour AS, Soden PD. Failure Criteria in Fibre Reinforced Polymer Composites: The World-Wide Failure Exercise. UK: Elsevier Ltd; 2004. ISBN: 978-0-08-044475-8

[4] Ballistic Resistance of Body Armor, NIJ Standard-0101.06, U.S. Department of Justice Office of Justice Programs National Institute of Justice; 2008

[5]   Department of Justice, National Institute of Justice. NIJ Standard 0108.01 US. Ballistic Resistant Protective Materials; September 1985

[6]   Montgomery JS, Chin ES. Protecting the future force: A new generation of metallic armors leads the way. AMPTIAC Quarterly. 2004;**8**(4):15-20

[7]   Cunniff PM. An analysis of the system effects in woven fabrics under ballistic impact. Textile Research Journal. 1992;**62**(9):495-509

[8]   Lakunin VY, Shablygin MV, Sklyarova GB, Tkacheva LV. Assortment and properties of aramid fibres manufactured by Kamenskvolokno Co. Fibre Chemistry. 2010;**42**(3)

[9]   Ballistics Teijin Aramid, Ballistics Material Handbook 38-1405/2012; 2012

[10]   National Research Council. Opportunities in Protection Materials Science and Technology for Future Army Applications. The National Academies Press; 2011. ISBN: 978-0-309-21285-4

[11]   Pirvu C, Ionescu TF, Deleanu L, Badea S. Simplified simulation of impact bullet—Stratified pack for restraining ballistic tests. In: 21st Innovative Manufacturing Engineering & Energy International Conference—IManE&E. Romania: MATEC Web Conf; Vol. 112; 2017. DOI: https://doi.org/10.1051/matecconf/201711206023

[12]   Grujicic M, Bell WC, Arakere G, He T, Xie X, Cheeseman BA. Development of a meso-scale material model for ballistic fabric and its use in flexible-armor protection systems. Journal of Materials Engineering and Performance. 2010;**19**(1):22-39

[13]   Grujicic M, Snipes J, Ramaswami S, Avuthu V, Yen CF, Cheeseman B. Unit-cell-based derivation of the material models for armor-grade composites with different architectures of ultra-high molecular-weight polyethylene fibers. International Journal of Structural Integrity. 2010;**7**(4):458-489. ISSN: 1757-9864

[14]   Pirvu C. Contribuții la studiul experimental și numeric al pachetelor de protecție balistică cu fibre aramidice [thesis]. Dunarea de Jos University Galati; 2015

[15]   Purushothaman A, Coimbatore G, Ramkumar SS. Soft body armor for law enforcement applications. Journal of Engineered Fibers and Fabrics. 2013;**8**:97-103

[16]   Safta I. Contribuții la studiul teoretic și experimental al mijloacelor individuale de protecție balistică [thesis]. Military Technical Academy Bucharest; 2011

[17]   Shockey DA, Erlich DC, Simons JW. Lightweight fragment barriers for commercial aircraft. In: The 18th International Symposium on Ballistics San Antonio; 1999

[18]   Chitrangad I. Hybrid Ballistic Fabric, Patent No. 5,187,003; 1993. Available from: http://www.freepatentsonline.com/5187003.pdf [Accessed: January 05, 2018]

[19]   Zeng XS, Shim VPW, Tan VBC. Influence of boundary conditions on the ballistic performance of high-strength fabric targets. International Journal of Impact Engineering. 2005;**32**(1–4):631-642

[20] Lim CT, Tan VBC, Cheong CH. Perforation of highstrength double-ply fabric system by varying shaped projectiles. International Journal of Impact Engineering. 2002;**27**(6):577-591

[21] Dischler L. Bullet Resistant Fabric and Method of Manufacture. U.S. Patent 6,248,676; 2002. Available from: http://www.google.com/patents/about?id=nGsIAAAAEBAJ&dq=Martin-Electronics&ie=ISO-8859-1 [Accessed: January 05, 2018]

[22] Carrillo JG, Gamboa RA, Flores-Johnson EA, Gonzalez-Chi PI. Ballistic performance of thermoplastic composite laminates made from aramid woven fabric and polypropylene matrix. Polymer Testing. 2012;**31**:512-519

[23] Bhatnagar A. Lightweight Ballistic Composites. Boca Raton Boston New York: CRC Press; 2006

[24] Allen SR, Filippov AG, Farris RJ, Thomas EL. Macrostructure and mechanical behavior of fibers of poly-p-phenylene benzobisthiazole. Journal of Applied Polymer Science. 1981;**26**(1):291-301

[25] de Koning CAM, Dreumel WHM. Mechanical Jointing in Aramid Fibre Composites. An Experimental Study, Report LR-371. Department of Aerospace Engineering. Delft University of Technology; 1983

[26] Martinez MA, Navarro C, Cortis R, Rodriguez J, Sanchez-Galvez V. Friction and Wear Behaviour of Kevlar Fabrics. Journal of Materials Science. Vol. 28. pp. 1305-1311. Springer. New York: Science + Business Media; 1993

[27] Al-Bastaki NMS. Design of fibre reinforced composite structures subjected to high strain rates using finite element analysis. Applied Composite Materials. 1998;**5**:223-236. Kluwer Academic Publishers

[28] Yahaya R, Sapuan SM, Jawaid M, Leman Z, Zainudin ES. Quasi-static penetration and ballistic properties of kenaf-aramid hybrid composites. Materials and Design 63. Elsevier Ltd; 2014. p. 775-782